# Morphology and growth characteristics of $Si_3N_4$ whiskers made by pyrolysis of amorphous Si–N–C powders

YA-LI LI[‡], YONG LIANG, ZHUANG-QI HU
*National Key Lab of Rapidly Solidified Nonequilibrium Alloys, Institute of Metal Research, Chinese Academy of Science, 72 Wenhua Road, Shenyang 110015, People's Republic of China*

The morphology and growth characteristics of $\alpha$-$Si_3N_4$ whiskers grown by pyrolysis of amorphous Si–N–C powders were investigated mainly by TEM. It was found that the whiskers exhibited various morphologies including ribbon-, rod-, prism- and nodule-like whiskers. Three growth directions were found: $\{1\bar{1}00\}^*$, $\{1010\}^*$ and $\{0001\}^*$ which are dense planes in the hexahedral structure of $\alpha$-$Si_3N_4$. No bobbles existed on the whisker tips, but there was a leading growth along the whisker long axial directions and small $Si_3N_4$ grains bonded on the whisker tips, which indicated that the whiskers nucleated on small $\alpha$-$Si_3N_4$ grains and grew by a vapour–solid condensation mechanism.

## 1. Introduction

With the development of high-performance ceramic and composite materials $Si_3N_4$ whiskers, as an important reinforcing material, have received extensive attention, because they have many superior physical, chemical and mechanical properties such as high thermal resistance, high toughness and strength, and large dielectrical constant [1], and the whiskers have a strength approaching the intrinsic values of the materials due to their single crystal characteristics. There has been much published work concerning the preparation of $Si_3N_4$ whiskers by various methods, which can be classified into silicon nitriding [2], carbothermal reaction [3], and halide gas reaction [4]. In our former paper, we reported an *in situ* synthesis of high-purity $\alpha$-$Si_3N_4$ whiskers from amorphous Si–N–C powders [5]. The *in situ* formation of the whisker indicates that there were different growth characteristics from those formed by the other methods mentioned above, in which a specific impurity nucleation site was generally needed for whisker growth by vapour–liquid–solid (VLS) mechanism [4].

A study of whisker morphology and structural characteristics is helpful to understand the whisker growth mechanism. The study is also important to provide information on the whisker's mechanical performance and to understand the crystal characteristics of $Si_3N_4$. However, less work has been conducted on the study of whisker morphology and structure characteristics in the past, except for the work done by Sasaki et al. [6] who studied the defects and growth characteristics of $Si_3N_4$ whiskers made by carbothermal reactions. In the present work, the morphology, structure and defects in the $\alpha$-$Si_3N_4$ whiskers produced by pyrolysis of amorphous Si–N–C powers were studied and the whisker growth mechanism was discussed.

## 2. Experimental procedure

$\alpha$-$Si_3N_4$ whiskers were synthesized from amorphous Si–N–C powders ($SiN_{0.5}C_{1.2}$) in a graphite resistance furnace at 1600° C and 1 atm nitrogen [5]. The whisker grew only on the original Si–N–C powder compacts indicating an *in situ* formation. X-ray diffraction (XRD) revealed that the only crystallized phase in the whiskers was $\alpha$-$Si_3N_4$. Typical scanning transmission electron microscopy (STEM) morphology of the whiskers produced is shown in Fig. 1. The whisker diameters changed from 0.05–1 μm and length changed from 0.5 μm to several millimetres, which is much longer than the presently commercially available $Si_3N_4$ whiskers [1].

The whisker morphology and structure were studied on Phillips TEM-420 transmission electron microscopy systems. The samples used for TEM observation were prepared by dispersing whiskers in alcohol followed by 1 h ultrasonic vibration, then dripping several drops of the dispersion on to copper grids coated with a layer of amorphous carbon.

## 3. Results and discussion

### 3.1. Whisker morphology

Careful TEM observation revealed that the whiskers, as shown in Fig. 1, consisted of various types of whiskers with different morphology as shown in Fig. 2. The first type of whisker has a smooth surface and rectangular cross-section with a large number of

[‡] Author to whom all correspondence should be addressed.

0022–2461 

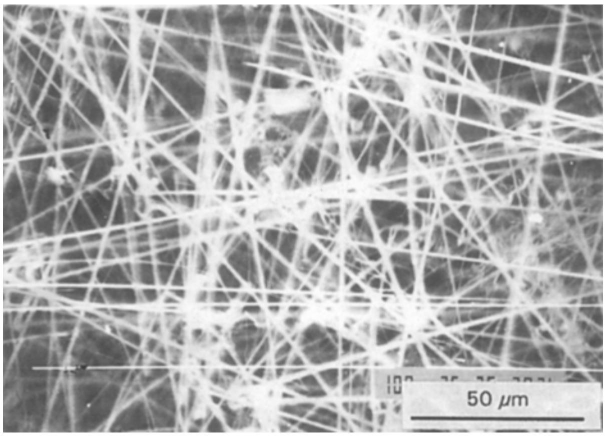


*Figure 1* Typical STEM morphology of α-$Si_3N_4$ whiskers produced from pyrolysis of nano-amorphous Si–N–C powders.

triangular defects on one side of the whiskers in the radial direction (see Fig. 2a and b). This type of whisker weighs about 80% of the total whiskers. Some twinned fringes crossing whisker radial directions with twinned $\{1\bar{1}01\}$ planes were occasionally observed (Fig. 2c). The dark-field image of Fig. 2c revealed the presence of many bulk defects in the whiskers, as shown in Fig. 2d. The morphology of the twinned fringes was very similar to that of silicon ribbons as observed by Greiner *et al.* [7] and Wagner and Treuting [8] who found that the silicon ribbons had twinned crystals with $\{111\}$ faces and a $\langle 112 \rangle$ long axis. In the present case, the twinned planes were perpendicular to the long growth directions.

The second type of whisker is the tape-like whisker as shown in Fig. 3a and b. This type of whisker was long (millimetres) and curled. The curling seems to be irregular, indicating that it formed during whisker growth. An explanation for the curling is that the whisker growth was hindered as the whisker front encountered solid particles in the Si–N–C compacts, which altered the whisker growth directions. The fact that the tap-like whiskers were mainly located in the lower part of the whisker supports the above explanation. Ge *et al.* studied the formation of $Si_3N_4$ whiskers and powders from imide, and stated that the whiskers formed when there was much space around the $Si_3N_4$ nuclei, and powdered $Si_3N_4$ formed due to the lack of free space for whisker growth [9]. Wang and Fischman [10] found that the SiC whisker morphology between the surface of the raw material compact and the bulk to be different, which was attributed to the difference in the degree of supersaturation and the availability of growth space.

The third type of whisker has prism morphology with a scale-like surface (Fig. 4a) or nodal-like morphologies (Fig. 3b and d). The whisker shown in Fig. 4b has many small crystals emerging from a whisker trunk having polycrystal characteristics as revealed by the dark-field image shown in Fig. 4c. Electron diffraction verified the whisker growth direction to be perpendicular to the $\{0001\}$ planes. The

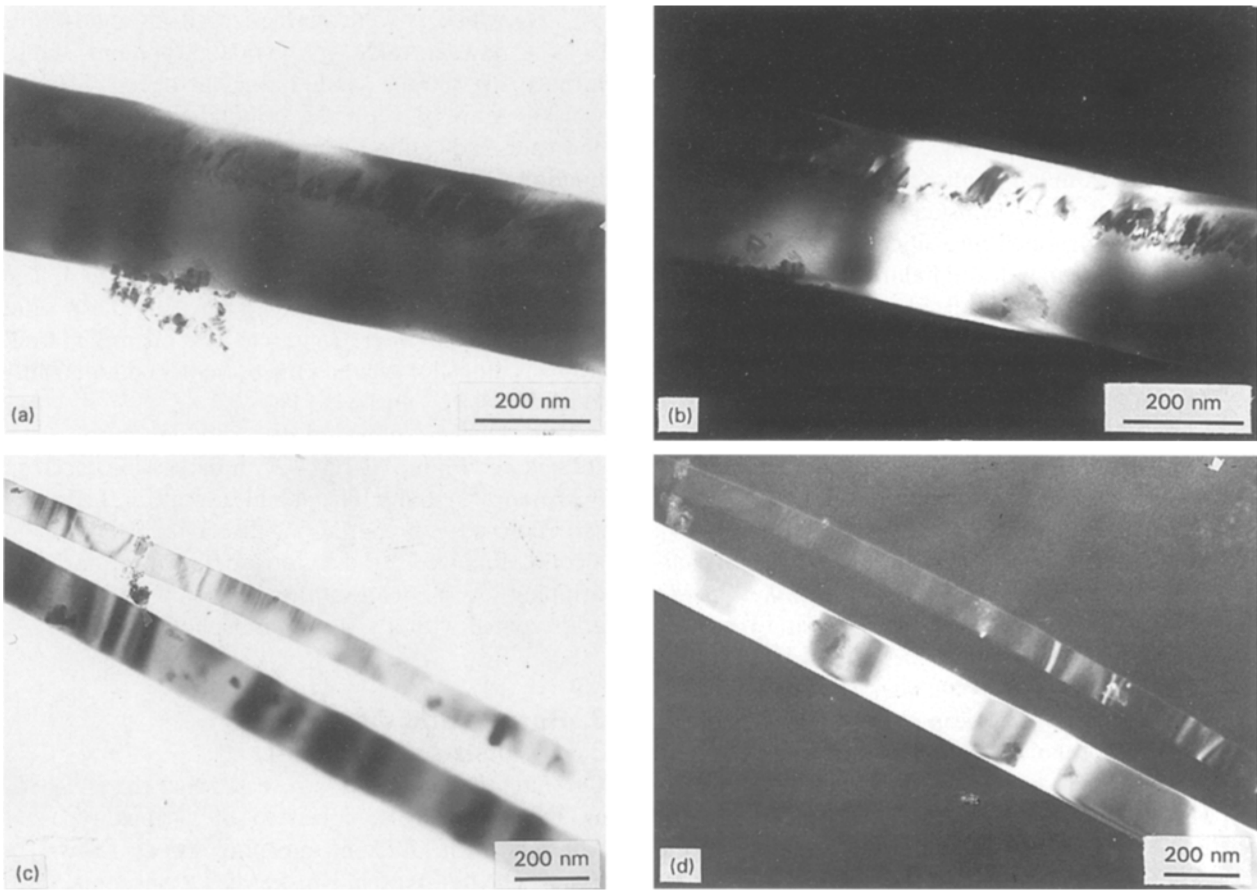


*Figure 2* TEM morphologies of straight, thick α-$Si_3N_4$ whiskers with rectangular cross-sections: (a) whiskers containing large amounts of small needle-like defects on one side, (b) dark-field image of (a), (c) twinned bands and bulk defects throughout the cross-section in the whiskers, (d) dark-field image of (c).

nodal whiskers shown in Fig. 4d seem to be formed by depleting $\alpha$-$Si_3N_4$ grains as the whisker growth front is attached to the grains, because the whiskers having this kind of morphology were more frequently found in the lower part of the whisker layer near to the raw

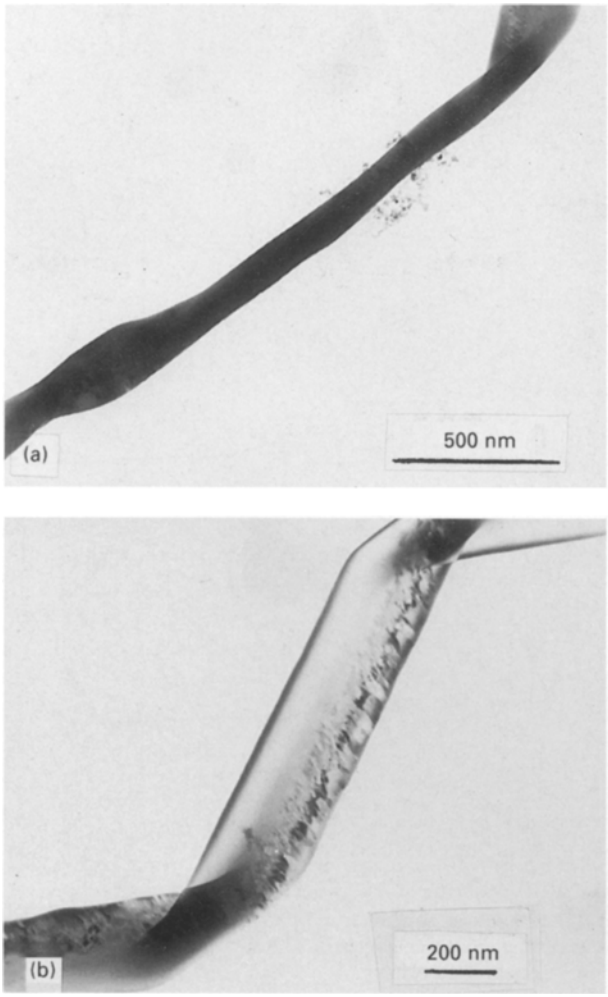


*Figure 3* TEM morphologies of the tap-like $\alpha$-$Si_3N_4$ whiskers: (a) the whiskers curled irregularly, (b) magnified view of (a) showing a large number of planar defects on one side of the whiskers.

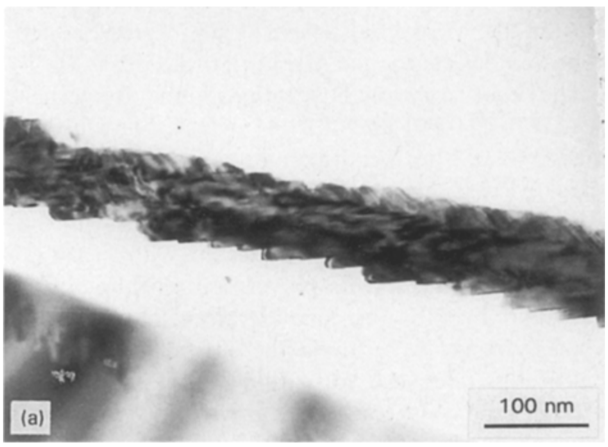


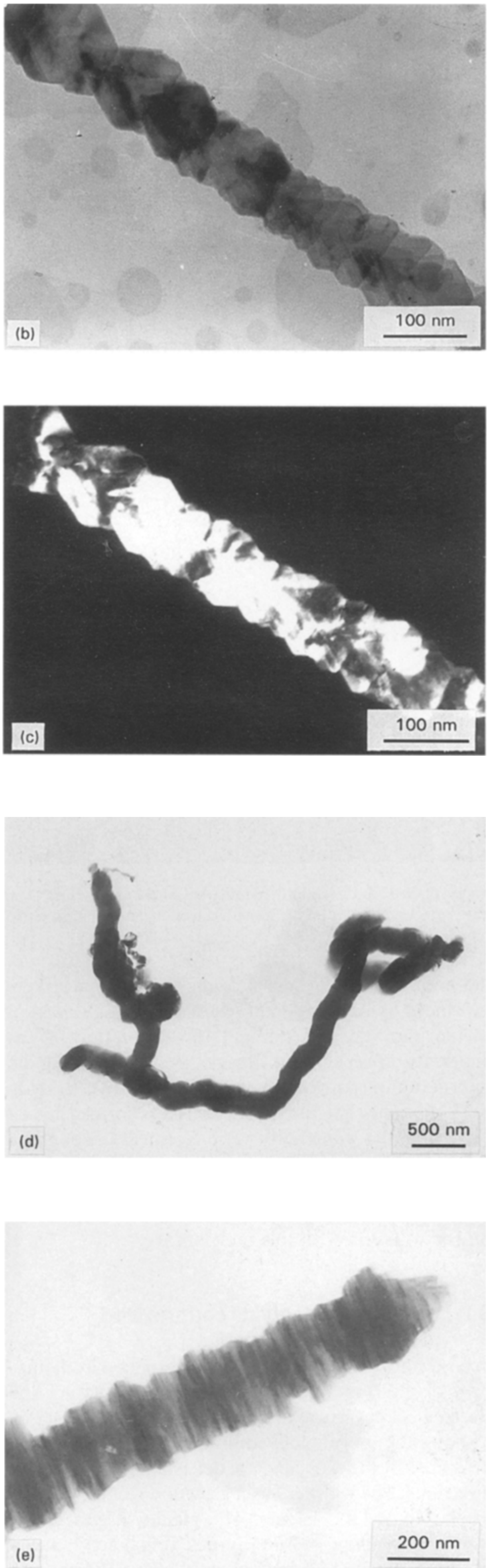


*Figure 4* TEM morphologies of the $\alpha$-$Si_3N_4$ whiskers with complex morphologies: (a) prism-like whiskers with triangular cross-sections and a scaley surface (growth direction $\{1\,0\,1\,0\}$*), (b) polycrystal whiskers containing many small grains emerging from the whisker trunk, (c) dark-field image of (b) showing the polycrystalline structure of the whiskers. (d) $\alpha$-$Si_3N_4$ whiskers with disordered structure along the axial directions.

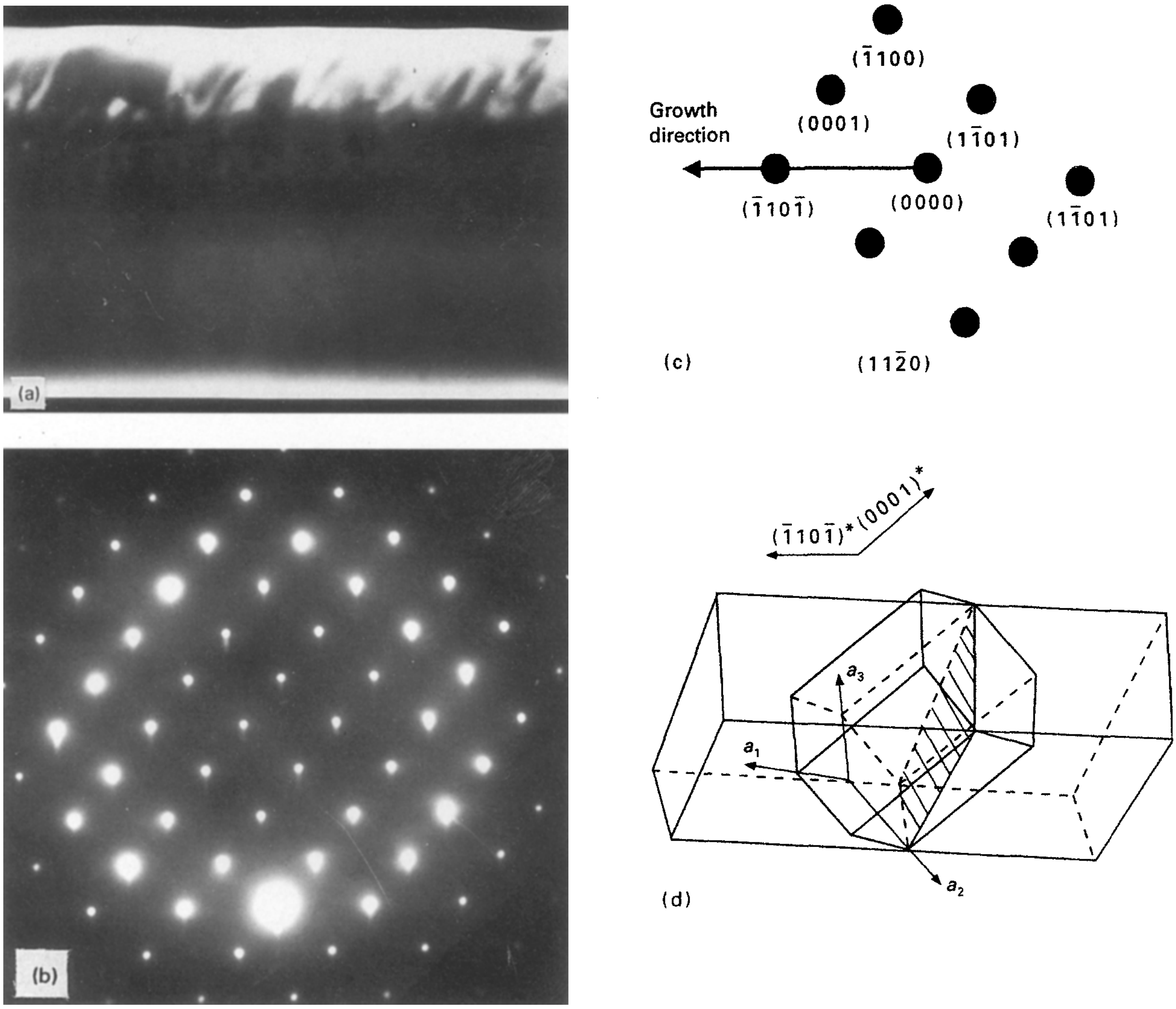


*Figure 5* Growth-direction determination of the thick, straight whiskers: (a) dark image of whisker morphology, (b) electron diffraction pattern, (c) calibration of the growth direction, and (d) schematic illustration of the growth characteristics of the whiskers.

material compact. Wang found $Si_2ON_2$ whiskers produced by carbothermal reactions having this kind of morphology, and thought the fluctuation of gas supersaturation allowed whisker growth following the alternation of particulates and whiskers [3]. Bi *et al.* [11] thought that the $Si_3N_4$ whiskers formed inside the $Si(NH)_2$ compacts were formed through a solid–liquid–solid (SLS) process. Fig. 4e shows the α-$Si_3N_4$ whiskers with disordered structure along the long axial direction. No detailed study was conducted on the whiskers with this morphology.

## 3.2. Whisker growth directions and growth characteristics

Whisker growth directions were determined from analysis of electron diffraction spots by regulating the electron beam vertical to the whisker outer surface. Fig. 5 shows the morphology, diffracting spots with beam directions of $\langle 1 1 \bar{2} 0\rangle$, and the determination of growth directions. The whisker has a growth direction perpendicular to $\{1 \bar{1} 0 1\}$ planes. The planar defects in the whiskers are along $\{0 0 0 1\}$ planes. It is noted that the planar defects are all located inside the whiskers and the outer surface is still smooth, as if coated with a layer of crystallites as shown by the dark-field image (Fig. 5a) obtained on a section of a $(1 \bar{1} 0 1)$ spot. This indicates that there was a subsequent growth in the radial direction after rapid growth along the long axial direction. The tap-like whiskers also have $\{1 \bar{1} 0 1\}^*$ growth directions and defects on one side of the whiskers.

The other two growth directions found are perpendicular to $\{1 0 1 0\}$ and $\{0 0 0 1\}$ planes. The whiskers with $\{1 0 1 0\}^*$ growth directions generally have a triangular cross-section in prism-like morphology, as shown in Fig. 4a. This result is in agreement with that of Sasaki *et al.* [6]. The whiskers with $\{0 0 0 1\}^*$ growth directions have a polycrystal morphology, as shown in Fig. 4b. The small grains emerging from whisker trunks were along the $\{0 0 0 1\}^*$ directions. Fig. 6 illustrates the formation mechanism of the whiskers: the whiskers grew along $\{0 0 0 1\}^*$ directions with subsequent slower growth along the six identical directions of $\{1 \bar{1} 0 1\}^*$.

From the above analysis, we know that the $Si_3N_4$ whiskers mainly grew along the densely arranged planes in the hexahedral structure of α-$Si_3N_4$, that is $\{1 \bar{1} 0 1\}$, $\{1 0 1 0\}$ and $\{0 0 0 1\}$ planes. This is in agreement with classical crystal growth theory that crystals grow along high-energy planes. Some authors

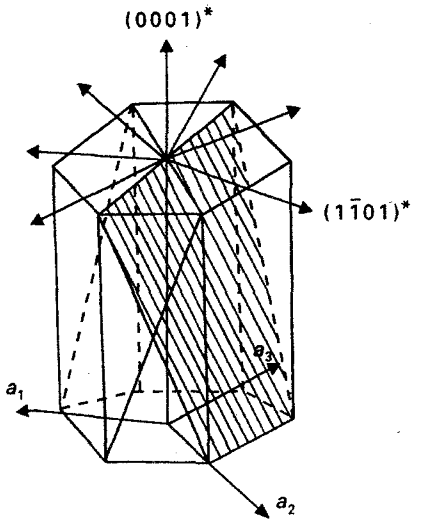


*Figure 6* Schematic illustration of the polycrystal whiskers with {0001} growth directions showing the emergence of $Si_3N_4$ grains from the whisker trunk along {1$\bar{1}$01}* directions.

reported a growth direction of ⟨101⟩ for $Si_3N_4$ whiskers [3] which seem to be confused by the representation of the growth directions, because the growth direction along {101} planes is not the ⟨101⟩ crystal direction but is the {101}* direction (or represented as ⟨210⟩). From the fact that various morphologies were exhibited by the whiskers, it is known that the whisker growth directions were affected by some dynamic factors, such as the interaction between the whisker growth front and the raw material particles, and the fluctuation of gas concentration.

### 3.3. Whisker growth mechanism

Whisker formation undergoes a nucleation and growth process. In the carbothermal process, the addition of catalysts such as iron or cobalt is necessary for providing a liquid phase with a low melting point for whisker impurity nucleation and growth along a specific crystal direction by the vapour–liquid–solid (VLS) mechanism, as illustrated in Fig. 7a. In the VLS process, the liquid droplets on whisker tips act as a liquid medium for mass transfer from vapour to solid, and the presence of condensed spherical droplets on whisker tips becomes evidence for identification of the VLS growth characteristic [12].

TEM observation revealed that there were no spherical droplets on whisker tips. The whisker tips are smooth as shown in Fig. 7a. However, small α-$Si_3N_4$ grains were frequently found bonded to one end of the whiskers, as shown in Fig. 7b. The absence of spherical droplets on whisker tips and the small grains bonded on the whiskers, indicate that the whiskers were formed directly from vapour condensation, and the whisker growth sites were α-$Si_3N_4$ grains. From Fig. 8b, it is also seen that one part of the whisker which originated from the $Si_3N_4$ crystallites is perfect and the other part contains a large number of planar defects. This indicates that the whisker section dimension is not exactly determined by the size of the nucleation grains. The defects on one side of the whiskers

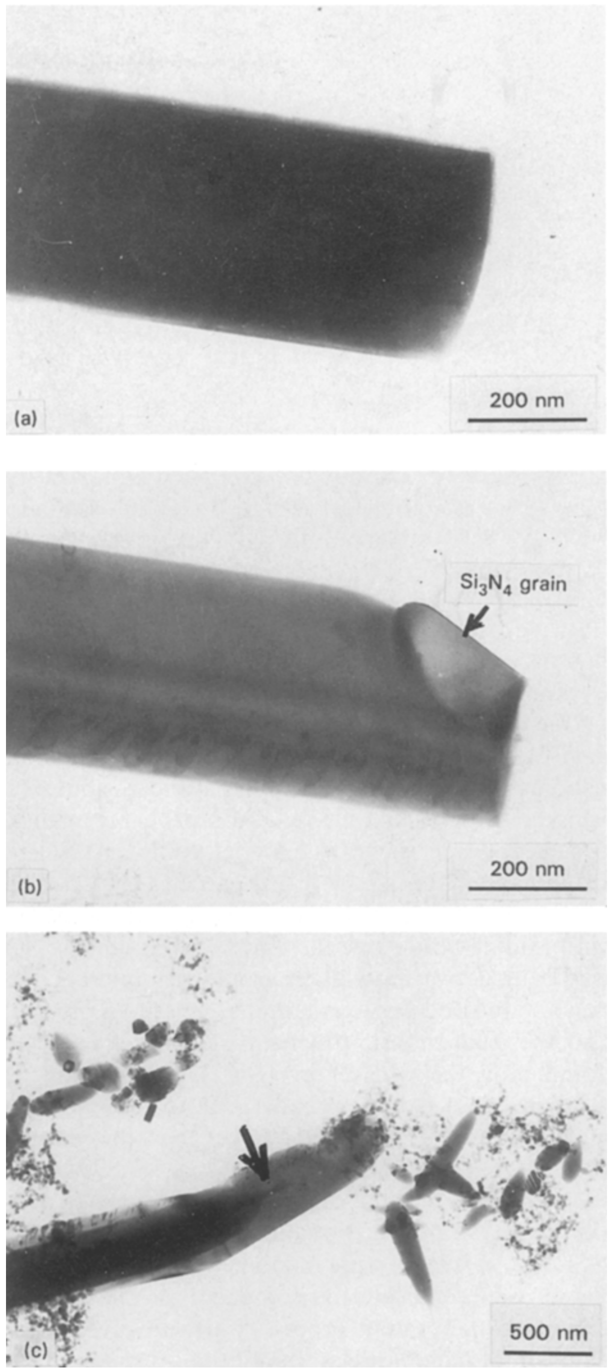


*Figure 7* (a) Leading growth and origin of whiskers from small crystallites; (b) whisker tips with small α-$Si_3N_4$ grains bonded on one end; (c) another smooth end of the same whiskers as in (b).

were formed during subsequent growth along perpendicular directions to the long axial directions. Wager and Treuting [7] found that the silicon ribbon width was mainly controlled by the nuclei size from which the ribbon originated.

Fig. 7c shows that there were thin needle-like whiskers present on the whisker tips (see the arrowed area in the figure). The presence of the leading growth indicates whisker growth by a screw dislocation mechanism: whisker growth by nucleation of gas molecules on the growth steps which existed at the whisker front. The fine particles, smaller than 30 nm in the figure, were α-$Si_3N_4$ which was revealed by SAD. Careful observation of the whiskers reveals there were some

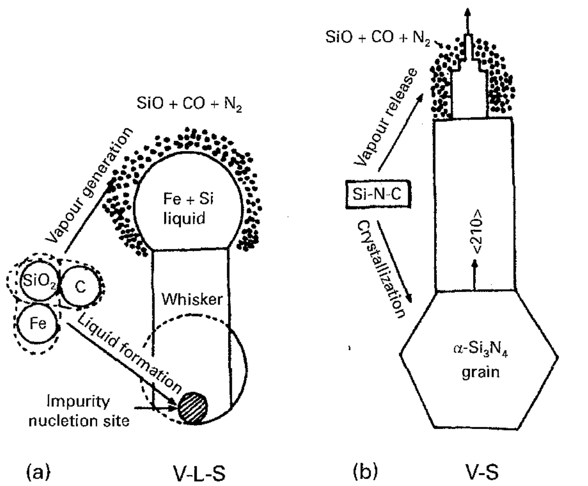


*Figure 8* Schematic illustrations of the whisker growth mechanism in (a) carbothermal reactions and (b) the pyrolysis of nano-amorphous Si–N–C powders.

fine particles diffused into the whiskers, and the defects on the one side of the whiskers seem to be caused by the depletion of the fine particles during whisker growth. This indicates that the solid diffusion of nanometre-sized α-$Si_3N_4$ particles also contributes to whisker growth, and this process probably mainly occurred inside the raw material compacts, where many nanometre-sized α-$Si_3N_4$ particles existed. The origination of the irregular whiskers from the whiskers with leading needle (see the thick whiskers in Fig. 7c) was caused by the whisker front encountering the nanometre-sized particles terminating the VS growth, and the solid diffusion of nanometre-sized particles dominating the whisker growth. The formation of a liquid phase is less probable, due to the synthesis temperature of 1873 K being lower than the melting point of the possible solid phase, such as $SiO_2$. The solid diffusion for whisker growth in our case is possible, because of the promoted diffusion rate of the α-$Si_3N_4$ particles with nanometre-sized particles. These results indicate the complicity of the whisker growth in the present process, which involved solid diffusion of nanoparticles in addition to the conventional VS growth by screw dislocations.

Fig. 8b shows a schematic illustration of the growth mechanism of the α-$Si_3N_4$ whiskers by pyrolysis of nano-amorphous Si–N–C powders. The α-$Si_3N_4$ grains for whisker nucleation resulted from the crystallization of the amorphous Si–N–C powders subjected to the correct SiO and CO pressure being attained in the systems. The release of SiO and CO vapour from Si–N–C powders occurred, accompanied by crystallization of the amorphous Si–N–C powders to produce α-$Si_3N_4$ particles. The SiO and CO gases were produced from the reaction of the surface oxide layer with carbon in the Si–N–C powders, because the Si–N–C powders contained an appreciable amount of surface oxygen (5–10 wt%) which came from air exposure. HTEM revealed there was an oxide layer about 5 nm thick on the Si–N–C particles of 50 nm diameter. The uniform distribution of oxide in a thin layer on the nanometric Si–N–C particle and the atomic distribution of carbon elements in the particles, avoid the retention of unreacted carbon or silica, which is often the case in the carbothermal reactions. The whisker nucleation on $Si_3N_4$ and growth by the VS mechanism without the addition of any catalyst, ensured *in situ* formation of the α-$Si_3N_4$ with high purity.

## 4. Conclusions

1. The α-$Si_3N_4$ whiskers produced from pyrolysis of nano-amorphous Si–N–C powders exhibited various morphologies, such as straight, thick whiskers with rectangular cross-sections, ribbon-like whiskers or nodal whiskers. The whiskers mainly grew along the three densely arranged planes that were $\{1\bar{1}01\}$, $(0101\}$ and $\{0001\}$.

2. The whiskers nucleated on $Si_3N_4$ grains formed from crystallization of Si–N–C powders and grew along the specific directions by the VS mechanism when the SiO and CO gases in the reaction system attained the correct concentration. Inside the Si–N–C compacts, the solid diffusion of nanometre-sized α-$Si_3N_4$ grains was also responsible for the whisker growth, which affected the whisker morphology and structure.

## References

1. K. NIWANO, in "Silicon Nitride-1", edited by S. Somiya, M. Mitomo and M. Yoshimura (Elsevier Applied Science, London, New York, 1989) p. 117.
2. Y. INOMATA and T. YAMANE, *J. Cryst. Growth* **21** (1974) 317.
3. M. J. WANG and H. WADA, *J. Mater. Sci.* **25** (1990) 1690.
4. K. KIJIMA, N. SETAKA and H. TANAKA, *J. Cryst. Growth* **24/25** (1974) 183.
5. Y.L. LI, Y. LIANG and Z.Q. HU, *Mater. Lett.* **21** (1994) 325.
6. K. SAKAKI, K. KURODA, T. IMURA and H. SAKA, *Yogyo-Kyokai-Shi* **94** (1986) 773.
7. E. S. GREINER, J. A. GUTOWSKI and W. ELLIS, *J. Appl. Phys.* **32** (1961) 2489.
8. R. S. WAGNER and R. G. TREUTING, *ibid.* **32** (1961) 2490.
9. C. GE, Y. XIA, J. XIE and X. HANG, in "4th International Symposium on Ceramic Materials and Components for Engines", edited by R. Carlsson, T. Johansson and L. Kahlman (Elsevier Applied Science, London, New York, 1990) p. 617.
10. HONGYU WANG and G. S. FISCHMAN, *J. Am. Ceram. Soc.* **74** (1991) 1519.
11. Y. BI, Z. YU and P. ZHANG, *Chin. Silica Bull.* **5** (1992) 53.
12. V. N. CRIBKOV, V. A. SILAVE, B. V. SCHETANOV, E. L. UMANTSEV and A. S. ISAIKIN, *Sov. Phys. Crystallogr.* **16** (1972) 852.

*Received 22 December 1994*
*and accepted 2 May 1995*